X-Ray Diffraction Study of Charge Density Waves in the Antiferromagnet $GdNiC_2$

X-ray diffraction measurements on $GdNiC_2$ have revealed intriguing behaviors originating from the interplay between charge density waves (CDWs) and magnetism. We found satellite peaks characterized by an incommensurate wave vector (0.5, η, 0) with η ≈ 0.52 below 205 K, suggesting the formation of a CDW. A transition to a commensurate phase with η = 0.5 occurs. The CDW lattice modulation is anomalously reduced below an antiferromagnetic transition temperature. Successive CDW transitions take place in magnetic fields. An incommensurate phase with (0.5, η, ζ) and that with (0.5, η, 0) are induced by magnetic fields. The CDWs disappear in coincidence with magnetic transitions in higher magnetic fields.

Low-dimensional systems exhibit noticeable properties, such as the charge density wave (CDW) and spin density wave. The CDW is a modulation of conduction electron density accompanied by a lattice modulation. Recently, much attention has been focused on $RNiC_2$ compounds (R denotes a rare-earth element), which show intriguing phenomena related to the interplay between CDWs and magnetism. The $RNiC_2$ compounds have an orthorhombic structure with the space group $Amm2$. For $SmNiC_2$, electrical resistivity and X-ray diffraction measurements revealed the emergence of the CDW characterized by the wave vector (0.5, η, 0) with η ≈ 0.52 below 148 K [1]. Destruction of the CDW occurs in coincidence with a ferromagnetic transition [1]. Investigations of the phenomena due to the interplay between CDWs and magnetism have led to an improved understanding of the interplay among different types of orders.

We have performed X-ray diffraction experiments on $GdNiC_2$ at BL-3A to investigate CDW phenomena and the effect of the antiferromagnetic order on the CDW [2]. Satellite peaks given by (0.5, η, 0) appear below T_1 = 205 K, at which the resistivity shows a sharp inflection. The temperature dependence of η is shown in **Fig. 1a**. The value of η varies with decreasing temperature, and then it locks into a commensurate value of 1/2 at T_{1C}. As shown in **Fig. 1b**, the intensity of the satellite peak decreases with decreasing temperature below the antiferromagnetic transition temperature (T_N), accompanied by the sharp decrease in the resistivity [2]. This means that the CDW lattice modulation is anomalously reduced below T_N. We observed diffuse scattering above T_1. The intensity distribution of the diffuse scattering has intensity maxima at the positions characterized by (0.5, η, 0) and (0.5, 0.5, 0.5), indicating the presence of soft phonon modes originating from CDW instabilities. Similar intensity distributions were observed in $SmNiC_2$ [1] and $TbNiC_2$ [2].

Figure 1c displays CDW and magnetic transition temperatures against the room temperature unit-cell volume in $GdNiC_2$, $SmNiC_2$, $TbNiC_2$, and other $RNiC_2$ compounds [2]. The CDW transition temperatures T_1 and T_{1C} appear to decrease with increasing unit-cell volume. Magnetic transitions have unfavorable effects on CDWs in $GdNiC_2$, $SmNiC_2$, and $TbNiC_2$. In $SmNiC_2$, the CDW order characterized by (0.5, η, 0) disappears below the ferromagnetic transition temperature (T_C). In $TbNiC_2$, the CDW satellite peaks given by (0.5, 0.5, 0) survive and those given by (0.5, 0.5, 0.5) disappear below T_N.

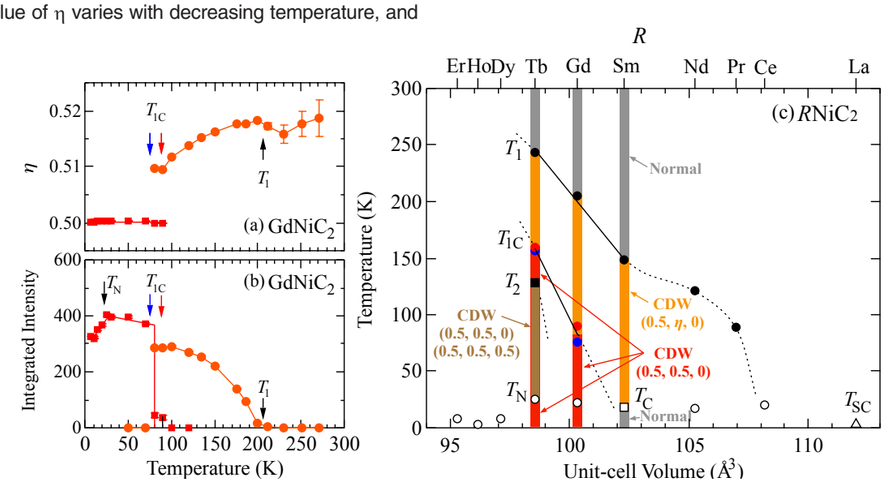

Figure 1: (a) Temperature dependences of **(a)** η and **(b)** integrated intensity of a satellite peak characterized by (0.5, η, 0) in $GdNiC_2$ [2]. **(c)** CDW transition temperatures plotted against the room temperature unit-cell volume in $RNiC_2$ [2].

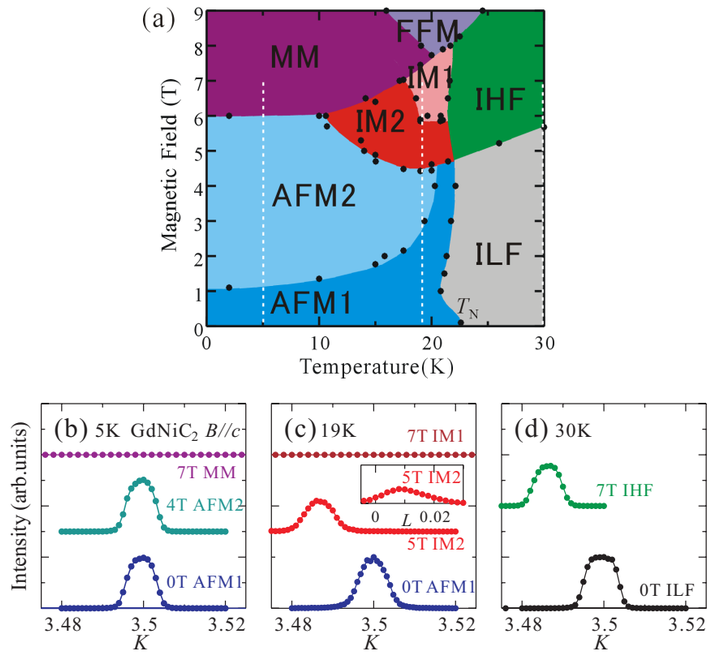

Figure 2: (a) Magnetic-field-temperature phase diagram of $GdNiC_2$ [3]. Magnetic-field dependence of satellite peak profiles observed at **(b)** 5 K, **(c)** 19 K, and **(d)** 30 K [3]. The magnetic field was applied parallel to the *c*-axis. The measurements of **(b)**, **(c)**, and **(d)** were performed under the condition indicated by the white dashed line in **(a)**.

The behavior of CDWs should be affected by external magnetic fields through the interplay between CDWs and magnetism. We have also performed X-ray diffraction experiments in magnetic fields at BL-3A. **Figure 2a** shows the magnetic-field-temperature phase diagram of $GdNiC_2$, determined by magnetization measurements in magnetic fields applied parallel to the *c*-axis [3]. Various magnetic and electronic states exist in the phase diagram. At 5 K (**Fig. 2b**), a CDW satellite peak given by (0.5, 0.5, 0) was observed in the antiferromagnetic phase 2 (AFM2 phase), which is the spin-flop state, as well as the antiferromagnetic phase 1 (AFM1 phase). The satellite peak disappears in the metamagnetic (MM) phase, in which the directions of the Gd moments are probably tilted toward the magnetic field. At 19 K, the intermediate phase 2 (IM2 phase) is stabilized above 4.5 T, and the satellite peak shifts its position toward an incommensurate position characterized by (0.5, η, ζ) as shown in **Fig. 2c**. The satellite peak disappears in the intermediate phase 1 (IM1 phase), where the magnetization value is close to half of the saturation moment. **Figure 2d** shows the satellite peak profiles above T_N. A field-induced commensurate-to-incommensurate phase transition takes place at the transition field from the ILF (intermediate-temperature–low-magnetic-field) to IHF (intermediate-temperature–high-magnetic-field) phase through the Zeeman effect. Successive transitions can be explained in terms of a cooperative effect of the Peierls instability and the spin Friedel oscillation [3]. The antiferromagnetic order of the *f* local moments is coupled to the spin density wave coexisting with the charge density modulation of the conduction electron. Here, the wave number of the antiferromagnetic order of the *f* local moments is assumed to coincide with the wave number ($2k_F$) of the density waves. When the *f* local moments are aligned by the magnetic field, the spin and charge density waves are suppressed through the exchange interaction.

REFERENCES

[1] S. Shimomura, C. Hayashi, G. Asaka, N. Wakabayashi, M. Mizumaki and H. Onodera, *Phys. Rev. Lett.* **102**, 076404 (2009).
[2] S. Shimomura, C. Hayashi, N. Hanasaki, K. Ohnuma, Y. Kobayashi, H. Nakao, M. Mizumaki and H. Onodera, *Phys. Rev. B* **93**, 165108 (2016).
[3] N. Hanasaki, S. Shimomura, K. Mikami, Y. Nogami, H. Nakao and H. Onodera, *Phys. Rev. B* **95**, 085103 (2017).

BEAMLINE

BL-3A

S. Shimomura[1], N. Hanasaki[2], C. Hayashi[3], Y. Kobayashi[3], H. Nakao[4], K. Mikami[5], Y. Nogami[5] and H. Onodera[6] ([1]Kyoto Sangyo Univ., [2]Osaka Univ., [3]Keio Univ., [4]KEK-IMSS-PF/CMRC, [5]Okayama Univ., [6]Tohoku Univ.)